

# Nickel pigmented anodized aluminium as solar selective absorbers

J. SALMI, J-P. BONINO, R. S. BES

*Laboratoire de Chimie des matériaux Inorganiques et Energétiques, ESA CNRS no. 5070, Université Paul Sabatier, 31062 Toulouse Cedex, France*

*E-mail: lme@ramses.ups-tlse.fr*

The effect of various impregnation parameters on the structural features and optical properties of solar absorbing nickel pigmented anodic alumina coatings has been studied. The impregnation starts from a threshold voltage. A correlation between microstructural features and the optical properties of these coatings has been established. Stable coating with low emissivity (0.14 at 70 °C) and high solar absorptivity (>0.90) have been prepared by anodizing in a phosphoric acid solution. © 2000 Kluwer Academic Publishers

## 1. Introduction

Selective surfaces for the photothermic conversion of solar energy can be obtained by chemical [1], physical [2] or electrochemical [3] conversion of stainless steel surface [4], zinc [5], copper [6] or aluminium [7]. In the case of aluminium alloys which are interesting for their lightness and their good capability towards shaping, a surface treatment process which involves a chemical composition modification of the anodic conversion layer by post processing was developed.

Conversion layers obtained through anodic oxidation of aluminium in an acidic electrolyte have physicochemical characteristics that depend on the electrolyte composition, the voltage applied, the temperature and the anodization duration [8]. The oxide coatings obtained by phosphoric anodic oxidation are composed of two parts consisting of a compact barrier layer and a layer of porous alumina of which pores are perpendicular to the aluminium surface [9]. By electrochemically including these porous films of metal particles, modified conversion layers are obtained and their original optical properties might lead to a development in the field of the photothermic conversion of solar energy. Selective absorber is a body having a spectral distribution near on the one hand to the distribution of a black body to absorb and on the other hand to the distribution of a metal polished to emit without having its reflective faculty. Selective absorber presents optical properties which are defined by the solar radiation total absorptivity  $\alpha_S$  and the total hemispherical emissivity  $\varepsilon_{70}$ . An ideal selective absorber would be a material that would absorb all the solar radiation without emitting. In practice a selective absorber can be considered good for  $\alpha_S \geq 0.95$  and  $\varepsilon_{70} \leq 0.20$ .

The influencing parameters of anodic oxidation are well-known [8] so we will focus our study on the second electrochemical stage of the process, i.e. impregnation by nickel particles.

Our goal is to study the physicochemical characteristics evolution of these coatings with respect to the

operating conditions and to correlate the latter with the covered surfaces optical properties.

## 2. Operating conditions

Used aluminium (99.5%) is shaped as rectangular sheet of 40 × 60 × 0.5 mm. Samples are initially degreased in a bath made up of sodium hydroxide, sodium carbonate, sodium métasilicate, trisodium phosphate and sodium gluconate during 1 min. This stage is followed by a sodium hydroxyde cleaning (25 g/l) during 1 min. The samples are then neutralised in a nitric acid bath (20% v/v) during 2 min. All these stages, carried out at ambient temperature, enable us to obtain a satisfactory surface quality before anodic oxidation.

Anodic oxidation is carried out in a phosphoric acid solution (0.5 M < X < 3 M), applied voltage of 15 V during 15 mn at a temperature of 20°C. After drying, the electrochemical impregnation under alternating voltage (50 Hz) is carried out in a nickel sulphate solution at ambient temperature.

The conversion layers Ni content ( $\mu\text{g}/\text{cm}^2$ ) is given by ionic chromatography DX100 with a column CS5. Structural characterisation is carried out by transmission electronic microscopy (T.E M). The concentrations of the elements in the impregnated anodization layer are followed by secondary ions mass spectroscopy (S.I.M.S). Optical properties  $\alpha_S$  and  $\varepsilon_{70}$  of conversions layers are measured using an absorptiometer and a emissiometer (EL 510-520 ELAN INFORMATIQUE).

## 3. Experimental results

### 3.1. Evolution of the optical properties

Evolution of the optical properties of nickel impregnated (10 min) anodic aluminium is shown on Fig. 1.

Absortivity starts only to increase above 5 V; below 5 V the optical properties are the same as the anodic aluminium layer ( $\alpha_S = 0.14$ ,  $\varepsilon_{70} = 0.08$ ).

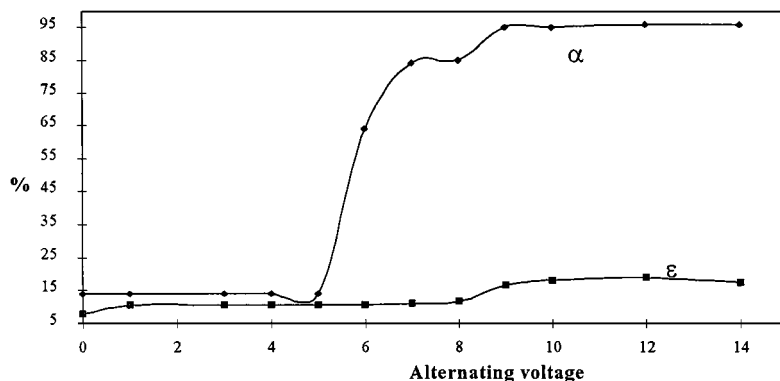


Figure 1 Absorptivity and emissivity in function of the applied alternating voltage.

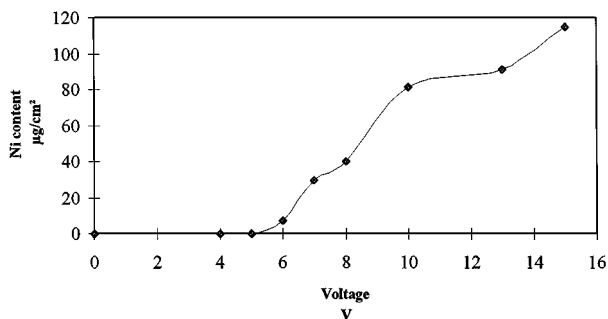


Figure 2 Ni content in function of the applied alternating voltage.

We obtain a good selective absorber when the applied alternating voltage reach 9 V. Fig. 2 gives the evolution of Ni content in the alumina layer according to the impregnating voltage. We can see that it is only at voltage in excess of a threshold voltage of 5 V that nickel is inserted. Thus, from comparison with Fig. 1, the increase in optical properties is associated with Ni.

However, above 9 V the Ni content does not have anymore impact on the evolution of the optical properties. Nickel insertion is a determining factor towards the obtention of good optical properties but above a given nickel content ( $60 \mu\text{g}/\text{cm}^2$ ), the optical properties do not evolve anymore.

### 3.2. Current signal analyse

In order to understand the evolution of nickel insertion with respect to applied voltage the evolution of current signal during impregnation was followed (Fig. 3).

For 4 V (Fig. 3a) a voltage for which nickel is not inserted in the alumina layer, we can observe symmetry between the anodic and cathodic parts.

When the voltage reaches 6 V (Fig. 3b) dissymmetry between the anodic and cathodic parts comes up with appearance in the cathodic field of a distortion due to the nickel reduction reaction. For higher voltages (Fig. 3c) the cathodic distortion increases and the cathodic field

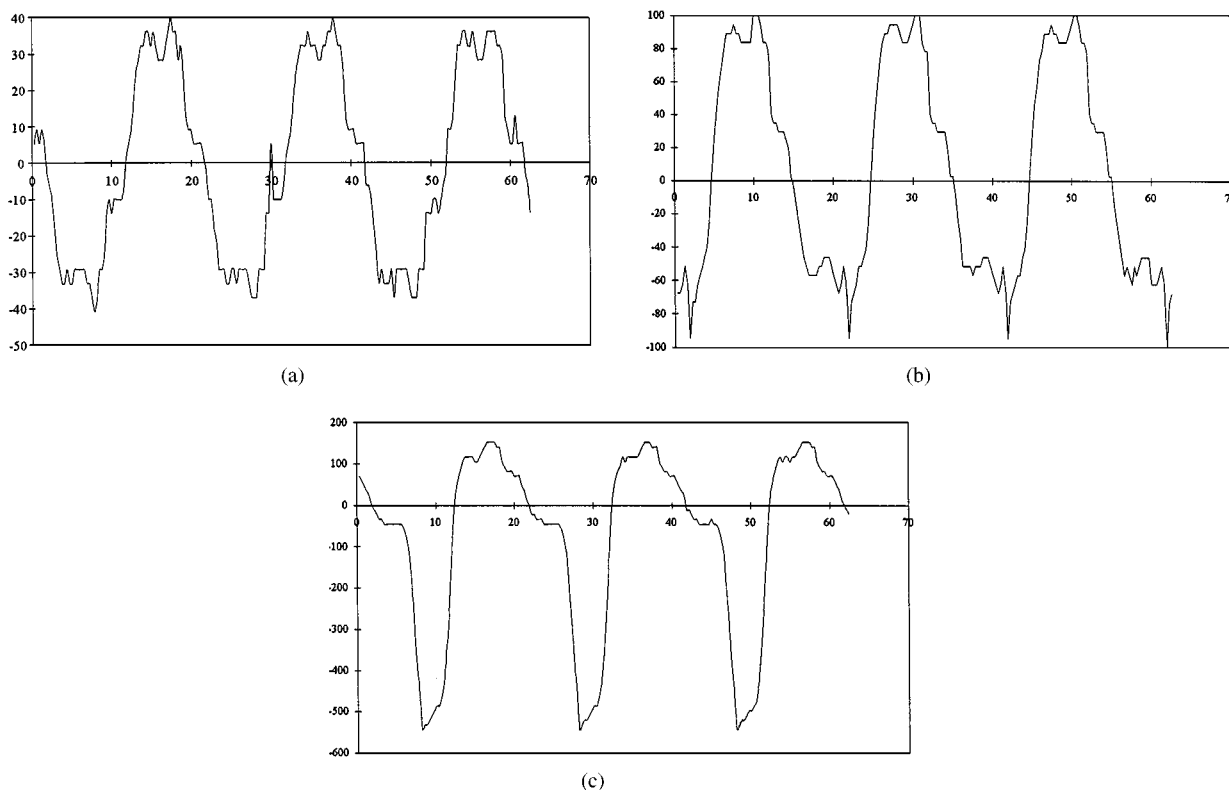


Figure 3 Current signal for various applied voltages (a) 4 V; (b) 6 V; (c) 10 V.

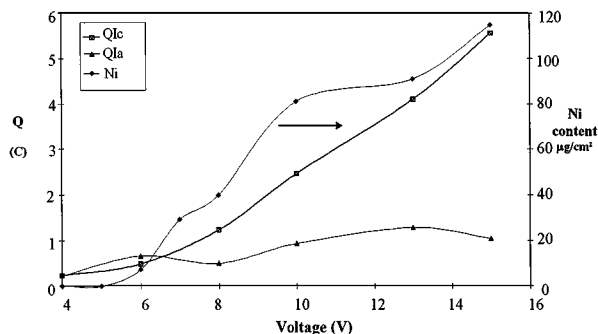


Figure 4 Current quantities according to the impregnation voltage.

becomes much larger than the anodic field. It corresponds to the fact observed on Fig. 2, i.e. the nickel content increases with the applied voltage. Indeed the cathodic field is the site of the nickel reduction reaction and the more this field become large, the more the nickel deposit is high.

Fig. 4, shows the evolution of current quantities in function of the applied voltage. We can see that anodic current quantity hardly vary when the voltage increase while the cathodic current quantity increase. When superimposing on these curves the evolution of the nickel content we can notice that the latter follows the cathodic current quantity.

From these curves we can say that the sole cathodic part plays a part in the nickel insertion but if the same experiment with d.c current is carried out, nickel forms a deposit on the surface and we have bad optical properties. Thus anodic field plays a role during the nickel insertion.

## 4. Deposit characterisation

### 4.1. S.I.M.S

When following the nickel profile as a function of applied voltage (Fig. 5a) we notice that for a small voltage (6 V) there is a bell-shaped profile; it means that nickel is located at the bottom of the pores of the alumina layer. When the voltage increases the deposited nickel increases and the pores fill up which is correlated by a flat S.I.M.S profile. The alumina layer can be estimated to  $0.40 \mu\text{m}$ . The threshold voltage is near to the product of the dielectric strength of alumina by thickness of the porous layer ( $\approx 5 \text{ V}$ ).

Assuming that the penetration speed of argon in the layer is constant for all the samples we can draw the curve of the pores filling rate in the alumina layer versus the voltage (Fig. 5b). For small impregnation voltages (6 V), the filling rate is 31% which shows that nickel is quickly inserted in the pores. Looking at the filling rate at which we have an optimum of selectivity (Fig. 1), we see that the rate is in the order of 42%. It shows that it is not necessary to completely fill the pores of the alumina layer to obtain good optical properties.

### 4.2. E.S.C.A

Carrying out a chemical analysis of elementary surface (Fig. 6) on an anodic sample (15 V, 15 min) and nickel

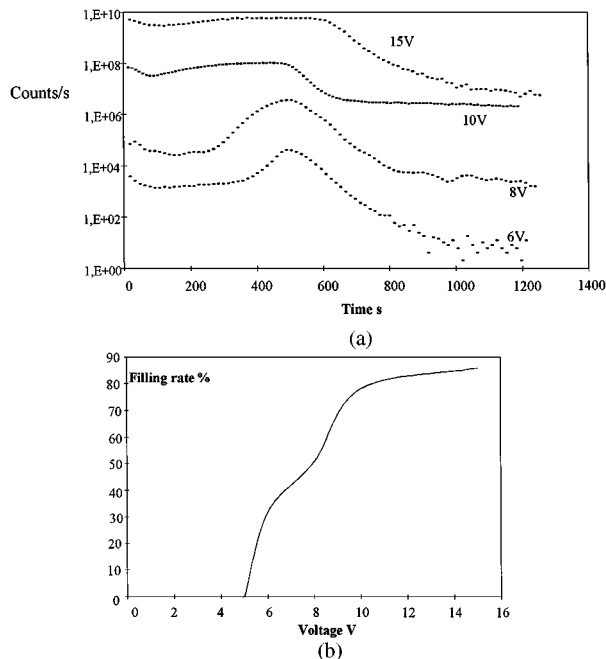


Figure 5 SIMS profiles (a) and filling rate (b) in fonction of applied voltage.

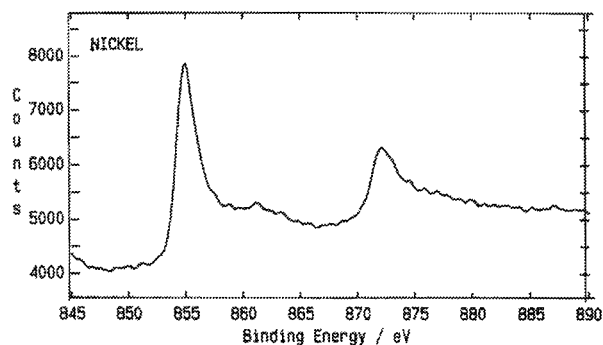


Figure 6 E.S.C.A analysis of the deposit.

impregnated (10 V, 10 min) we find two peaks located at 855 and 873 eV that respectively represent  $\text{Ni}(2\text{P}_{3/2})$  and  $\text{Ni}(2\text{P}_{1/2})$ . The nickel located at the bottom of the pores is in metallic form; nickel oxide  $\text{NiO}$  cannot be found in contrast to the report done by Kumar [8].

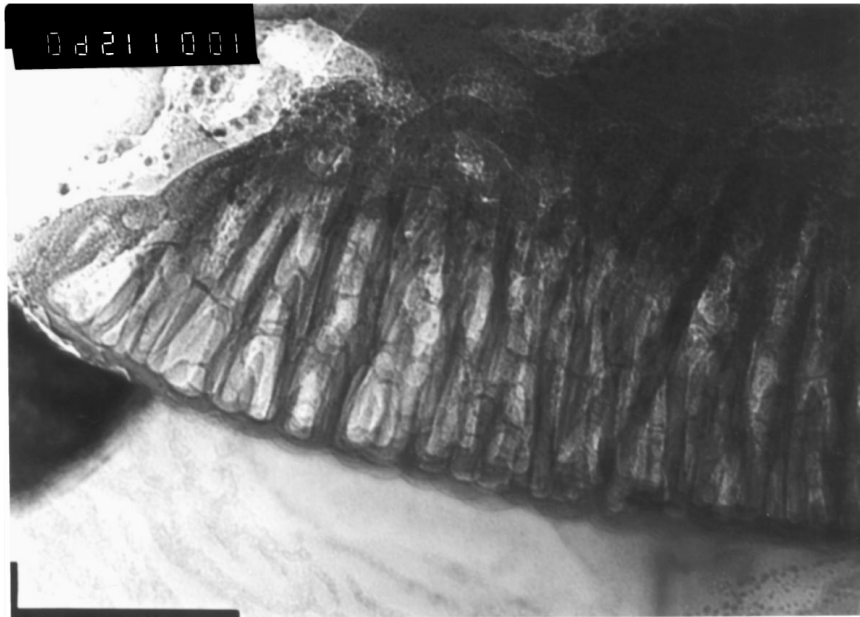
### 4.3. T.E.M

Before impregnation (Fig. 7a), the alumina layer of approximately  $0.40 \mu\text{m}$  thick consist' of pores, perpendicular to surface, which have an average diameter of 20 nm. The barrier layer that separates aluminium from the porous layer is 26 nm thick. After a 10 min impregnation under 10 V (Fig. 7b), the alumina layer fills up and we can see metallic nickel in the pores (black spots).

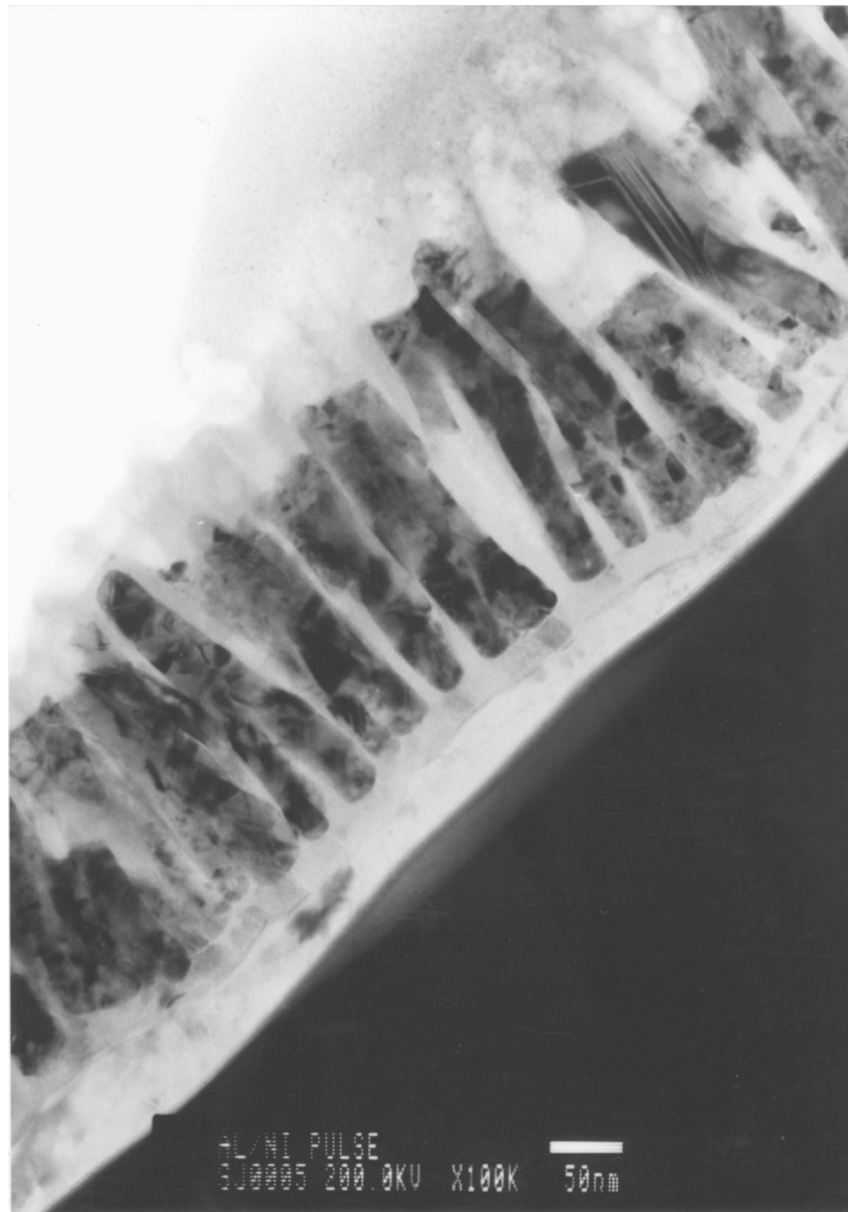
To supplement what we have observed by ESCA analysis, a diffraction on nickel present in the pores was undertaken. Rings of diffraction are obtained, and working out the spacings of these plans we find that they are close to the theoretical d spacings of nickel.

The nickel is microdivided in the pores of the alumina layer; this explains why it was not visible with X-rays.

Nickel being only present at the bottom of the pores makes it possible to obtain good optical properties



(a)



(b)

Figure 7 T.E.M photographs of anodically oxidised aluminium prepared in phosphoric acid solution before impregnation (a) and after impregnation (b).

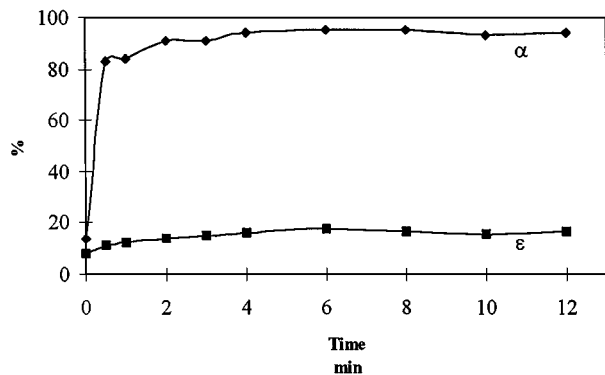


Figure 8 Absorptivity and emissivity in function of the impregnation duration.

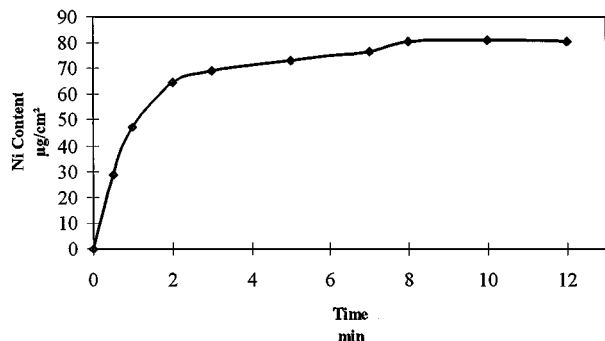


Figure 9 Ni content in function of the impregnation duration.

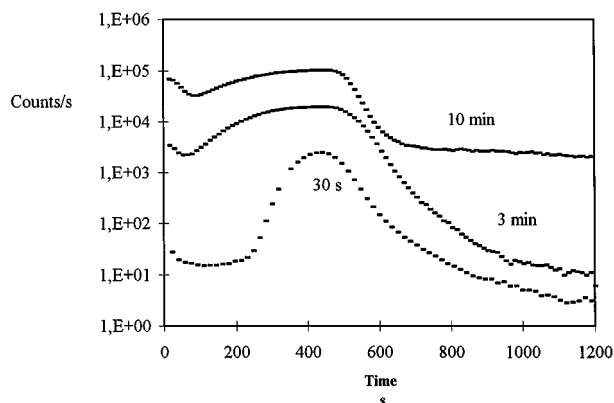


Figure 10 SIMS profiles in fonction of the impregnation duration.

without completely fill the pores with nickel. In order to check the relation made between a good selectivity and the presence of nickel at the bottom of the pores we vary the impregnation duration.

## 5. Impregnation duration

A short impregnation duration (2 min), for a process voltage of 10 V, is enough to obtain good optical properties (Fig. 8). On Fig. 9, we can notice that nickel is rapidly inserted: so after 2 min, a plateau between 70 and 80  $\mu\text{g}/\text{cm}^2$  is reached.

If a S.I.M.S study is undertaken for different impregnation duration (Fig. 10), we note that when the impregnation time is increased the nickel profile is flattened (the pores fill up) and does not evolve any more which corresponds to the plateau observed on Fig. 9. The pore filling of the alumina layer by nickel is made the pore bottom to the pore top.

## 6. Conclusion

Nickel insertion in the porous alumina layer starts from a threshold alternating voltage. Inserted nickel is in metallic form and is microdivided. The anodic composing of the signal plays a major part on the nickel insertion in the pores. The optical properties depend on the nickel content but a small content is sufficient to have good optical properties. It is not necessary to have nickel all along the pores, its sole presence at the pores bottom enable us to obtain a strong absorptivity and a low emissivity.

## References

1. S. KONATÉ, R. S. BES and J. P. TRAVERSE, *Ann. Chim. Sci. Mat.* **22** (1997) 67.
2. F. TROMBE, A. LEPHAT VINH and M. LEPHAT VINH, *J. Rech. CNRS* **65** (1964) 563.
3. H. M. BELGHITH, R. S. BES and J. P. TRAVERSE, French Patent no. 9508090, 3 juillet 1995.
4. L. ARIES, F. BERREKHIS, R. BENAVENTE, J. P. BONINO and J. P. TRAVERSE, *Mat. Res. Bull.* **18** (1983) 1113.
5. S. KONATÉ, Thèse, Université Paul Sabatier, Toulouse, France, 1997.
6. H. M. BELGHITH, Thèse, Université Paul Sabatier, Toulouse, France, 1995.
7. C. G. GRANQVIST, A. ANDERSON and O. HUNDERI, *Appl. Phys. Lett.* **35** (1979) 268.
8. S. N. KUMAR, L. K. MALHOTRA and K. L. CHOPRA, *Solar Energy Materials* **7** (1983) 439.
9. T. PAVLOVIC and IGNATIEV, *Thin Solid Films* **138** (1986) 97.

Received 20 May  
and accepted 22 July 1999